KIEL-UP • DOI: 10.38072/2748-3150/p38

Atmospheric cosmic ray induced ionization and radiation affecting aviation

Panagiota Makrantoni [1], Anastasia Tezari [2], Argyris N. Stassinakis [1], Pavlos Paschalis [1], Maria Gerontidou [1], Helen Mavromichalaki [1], Ilya G. Usoskin [3], Norma Crosby [4], Mark Dierckxsens [4]

Correspondence

1 Athens Cosmic Ray Group, Faculty of Physics, National and Kapodistrian University of Athens, Greece, pmakrantoni@phys.uoa.gr, a-stasinakis@phys.uoa.gr, ppaschalis@phys.uoa.gr, mgeront@phys.uoa.gr, emavromi@phys.uoa.gr

2 Eugenides Foundation, Athens, Greece, anatez@med.uoa.gr

3 Space Physics and Astronomy Research Unit and Sodankylä Geophysical Observatory, University of Oulu, Finland, ilya.usoskin@oulu.fi

4 Royal Belgian Institute for Space Aeronomy, Brussels, Belgium, Norma.Crosby@aeronomie.be, Mark.Dierckxsens@aeronomie.be

Keywords

cosmic rays; atmosphere; ionization; radiation; solar cycle; flight level; aviation

Abstract

Cosmic radiation is a major factor of ionization of the Earth's atmosphere. Both solar and galactic cosmic rays, which depend on solar activity and geomagnetic field, affect the radiation exposure in the atmosphere. Several models have been created for the estimation of the ionization and radiation dosimetry. In this work, as regards the ionization rate computations the CRAC:CRII model by the University of Oulu (https://cosmicrays.oulu.fi/CRII/CRII.html) was used, while for the estimation of the ambient equivalent dose rate (dH*(10)/dt) we used the validated software DYASTIMA / DYASTIMA-R by the University of Athens (http://cosray.phys.uoa.gr/index.php/applications/dyastima). Both tools are of great importance as they allow us to calculate the respective quantities all over the globe, at the entire atmosphere and for different time periods and solar cycle phases. The study concerns the last two solar cycles 23 and 24 (1996–2019) and specific flight levels of commercial aviation (FL310, FL350 and FL390). The dependance of CRII and dH*(10)/dt on geomagnetic cut-off rigidity, solar activity, cosmic ray intensity, as well as the altitude inside the atmosphere, affect the radiation exposure of the air crew members and frequent flyers, which make the results very interesting for the aviation industry.

KIEL-UP • DOI: 10.38072/2748-3150/p38

1. Introduction

Cosmic rays are highly energetic particles of extraterrestrial origin, with two main components, Galactic Cosmic Rays (GCR) which originate from outside of our Solar System and Solar Energetic Particles (SEPs) which are accelerated during eruptive processes on the Sun. As cosmic rays travel through the interplanetary space, they reach and penetrate the Earth's atmosphere, colliding with nuclei of atoms and ions of the atmosphere, creating nucleonic, muonic and electromagnetic cascades named secondary cosmic rays. Primary particles are absorbed inside the atmosphere due to ionization losses. In this way, cosmic rays affect the physical–chemical properties of the atmosphere. The Earth's magnetic field acts as a charge discriminator and modulates the cosmic ray flux that reaches each location on the Earth.

Cosmic rays contribute significantly to the atmospheric ionization (Cosmic Ray Induced Ionization – CRII). CRII is affected by the GCR and the 11-year solar cycle. Specifically, CRII is anti-correlated with the solar activity, while a significant dependance on SEPs is also observed at high latitude regions, at high altitude (Usoskin et al. 2009). The CRII may affect the Earth's climate, as many studies suggest that CRII may affect in numerous ways different climate parameters such as cloud cover, precipitation, cyclogenesis in mid- to high-latitude regions atmospheric transparency aerosol formation (Bazilevskaya et al. 2008, and references therein), the avionic electronic systems, as well as the human health of aircrews and / or passengers (Berger et al. 2008; Flückiger and Bütikofer 2011).

The major contributor to the aircrews' health is the occupational exposure to the ionizing cosmic radiation, during the flights. Aircrews and passengers are constantly exposed to the permanent GCR background, as well as to the unpredictable SEPs. Similarly, to the CRII, the radiation exposure is greater during conditions of minimum solar activity, as well as during strong events (SEPs, ground level enhancements – GLEs). For this reason, the radiation assessment of aircrews is of great importance and it can be performed by using several software tools and models.

The purpose of this work is the calculation of the CRII and the estimation of the radiation exposure of aircrews for different flying levels and different periods of solar activity. In order to perform the aforementioned calculations, the CRAC:CRII model and the DYASTIMA software have been used respectively.

2. Technical analysis and data selection

Regarding the calculations of the Cosmic Ray Induced Ionization (CRII) the CRAC:CRII model of the University of Oulu was used. CRAC:CRII is a numerical model, based on the CORSIKA code and the FLUKA Monte Carlo package, which allows extensive calculations of CRII from the Earth's surface to the upper limit of the atmosphere for every location on Earth. The computations derived from the model coincide with direct fragmentary measurements of the ionization in the atmosphere in a full range of parameters, covering all latitudes and altitudes during different solar cycle phases confirming its reliability and validity. Full details of the CRAC:CRII model are given in Usoskin and Kovaltsov (2006) and Usoskin et al. (2010).

For the calculations of the ambient dose equivalent rate $dH^*(10)/dt$, the Dynamic Atmospheric Shower Tracking Interactive Model Application (DYASTIMA) of the National and Kapodistrian University of Athens was used. The DYASTIMA software is based on Monte Carlo simulation techniques using the Geant4 toolkit (Agostinelli et al. 2003; Allison et al. 2006, 2016). It simulates air showers and cosmic ray secondary

KIEL-UP • DOI: 10.38072/2748-3150/p38

particles cascades inside the atmosphere of a planet and it is a federated product on the ESA SWE Portal (https://swe.ssa.esa.int/dyastima-federated), validated according to ICRP / ICRU criteria (ICRP 2007, 2016; ICRU Report 84 2010; ESA 2019). Moreover, the radiobiological quantities were calculated with the DYASTIMA-R extension. The full details of DYASTIMA software are given in Paschalis et al. (2014) and the DYASTIMA Software User Manual (2019).

The input parameters required for the DYASTIMA / DYASTIMA-R software are the characteristics of the planet and its atmosphere, we used the International Standard Atmosphere (ISA) model (ISO 2533:1975ISO 2007), the differential spectrum of the incoming primary cosmic ray particles at the top of the atmosphere, the ISO15390 model was used (ISO 15390:2004ISO, 2004), the appropriate physics list, the FTFP_BERT_HP GEANT4 list was used, the magnetic field components, obtained from the National Oceanic and Atmospheric Administration (NOAA) portal (https://www.ngdc.noaa.gov/geomag/), the particle detection altitudes and the settings concerning the realization of dosimetric calculations.

3. Results

In this work, both the CRAC:CRII model and the DYASTIMA/DYASTIMA-R software were applied globally, from cut-off rigidity 0-17 GV, during the last two solar cycles 23 and 24, i.e. years 1996-2008, 2009-2019, and were focused on specific altitudes that correspond to the most common commercial flight levels, i.e. FL310 (9.45 km a.s.l.), FL350 (10.67 km a.s.l.), FL390 (11.89 km a.s.l.).

The results obtained are depicted on maps. Figure 1 shows the CRII rate, globally, during the solar minima and maxima of the last two solar cycles, SC23 (1996-2008) and SC24 (2009-2019), at FL390, while Figure 2 and 3 show the same quantities for FL350 and FL310 respectively. It is obvious that the CRII rate was greater during the solar minima than during the solar maxima for both solar cycles 23 and 24. This fact is due to the CRII following the cosmic ray intensity behavior with which it is positively correlated, while it is negatively correlated with the solar activity. This means that the greater the solar activity, the lower the intensity of the CRII and vice versa (Forbush 1954; Gleeson and Axford 1968; Mavromichalaki et al. 1998; Makrantoni et al. 2013, 2021, 2022).

Moreover, if we compare the values of solar cycles 23 and 24, it is clear that during both the solar minima and maxima they were greater during solar cycle 24 than these of solar cycle 23. This coincides with the fact that solar cycle 24 was a quiet solar cycle, while solar cycle 23 was a very active one. As depicted on the maps, it is observed that, at polar regions the ionization rate has maximum values, while at equatorial regions, the ionization rate has minimum values. Responsible for this is the magnetic field of the Earth and thus the different geomagnetic cut-off rigidity (R_c) that corresponds to each location. At polar regions, where the geomagnetic cut-off rigidity is lower (R_c=0 GV), more cosmic rays penetrate the magnetosphere and the atmosphere of the Earth, which lead to atmospheric ionization, than at equatorial regions, where the geomagnetic cut-off rigidity is greater (R_c=17 GV). All the aforementioned maps were generated via the rigidity maps of Smart and Shea (2007a; 2007b; 2019) and (Gerontidou et al. 2021).

Comparing the maps for FL390 in Figure 1, with the respective maps for FL350 in Figure 2 and FL310 in Figure 3, it is evident that the CRII rate significantly increases with altitude, as expected up to the Regener-Pfotzer maximum. More to that, the same pattern between the two solar cycles is observed; the CRII rate is higher during solar cycle 24 where the solar activity is lower.

KIEL-UP • DOI: 10.38072/2748-3150/p38

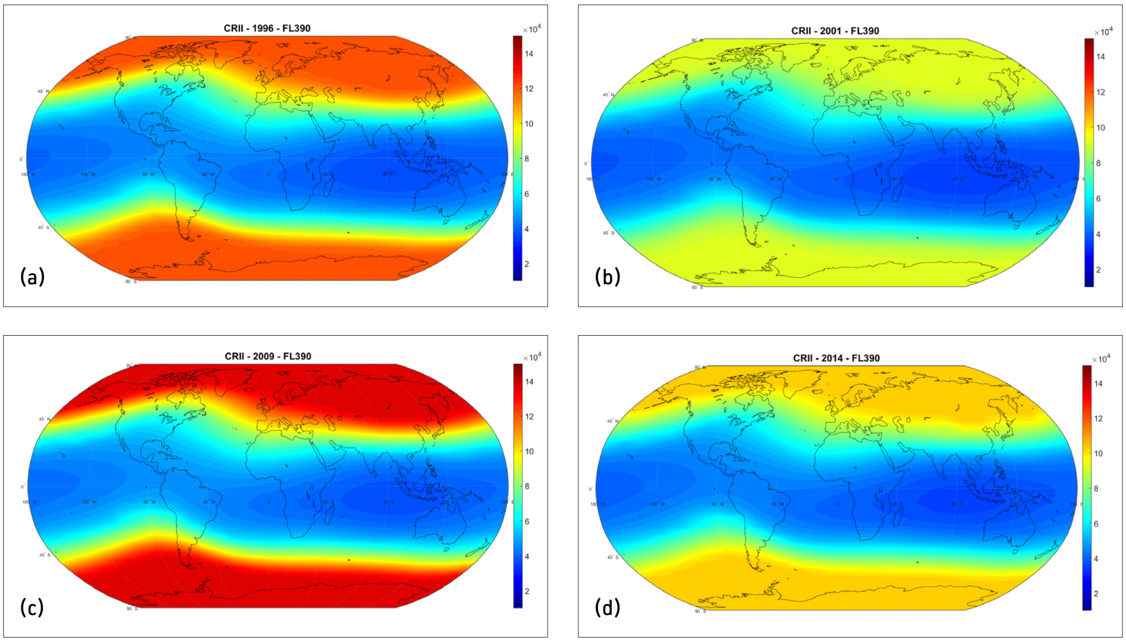

Fig. 1: Maps of CRII rate (ion pairs/(g*s)) at FL390: (a) during the minimum of solar cycle 23; (b) during the maximum of solar cycle 23; (c) during the minimum of solar cycle 24; (d) during the maximum of solar cycle 24.

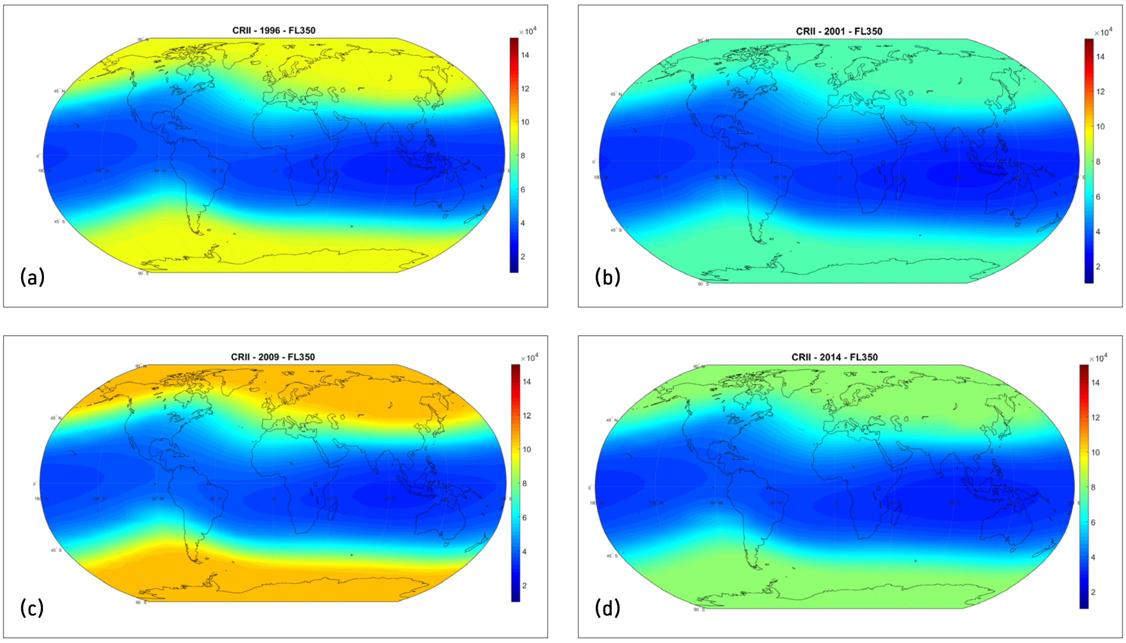

Fig. 2: Maps of CRII rate (ion pairs/(g*s)) at FL350: (a) during the minimum of solar cycle 23; (b) during the maximum of solar cycle 23; (c) during the minimum of solar cycle 24; (d) during the maximum of solar cycle 24.

The ambient dose equivalent rate during the solar minimum and maximum of solar cycle 23 at all three FLs is presented in Figures 4 and 5 respectively. The dependence of the radiation levels on the cosmic ray intensity at the different atmospheric altitudes (Tezari et al. 2020, 2022), eventuates in the dH*(10)/dt behaving the same way as CRII does, i.e., minimum values are found at equatorial regions

KIEL-UP • DOI: 10.38072/2748-3150/p38

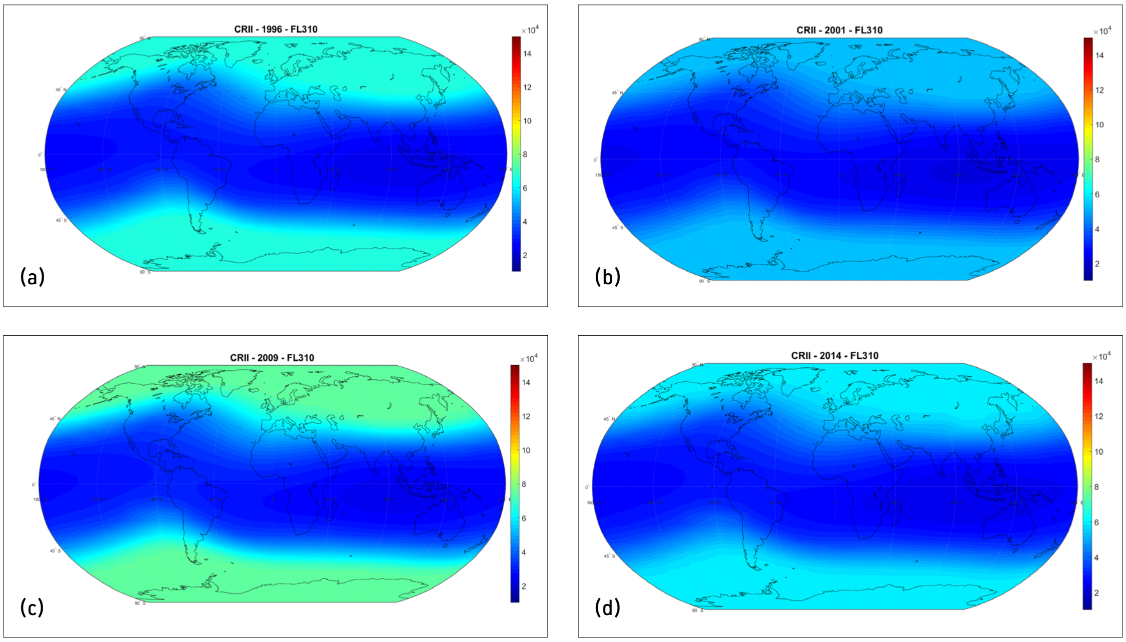

Fig. 3: Maps of CRII rate (ion pairs/(g*s)) at FL310: (a) during the minimum of solar cycle 23; (b) during the maximum of solar cycle 23; (c) during the minimum of solar cycle 24; (d) during the maximum of solar cycle 24.

(R_c=15-17 GV) whereas maximum values at polar regions (R_c=0-2 GV). Furthermore, it is observed that the radiation exposure during the solar minimum was greater than that during the solar maximum, due to the negative correlation between the intensity of the incoming cosmic ray particles and the solar activity. Once again, comparing the maps of the three flight levels, it is evident that the ambient dose equivalent rate also significantly increases with altitude.

Figure 6 presents time profiles of the annual values of CRII rate and ambient dose equivalent rate for the same period of time (year 1996 to 2019) for the three typical FLs and for four different geomagnetic cut-off rigidities (0.1 GV, 3.1 GV, 8.5 GV and 14.9 GV). It is observed that both CRII rate (blue lines, left axis) and ambient dose equivalent rate (red lines, right axis) follow an 11-year modulation, at all the locations, the same way the Galactic Cosmic Ray intensity does (Makrantoni et al. 2021, 2022; Tezari et al. 2022; Mavromichalaki et al. 1995), as the intensity of the cosmic radiation directly affects the radiation exposure of the aircrew.

Moreover, as regards the time profiles of the three different flight levels, we observe that the CRII and ambient dose equivalent rates increase as the flight level of the aircraft increases. This is due to the fact that the shielding effect of the atmosphere reduces with height and consequently the radiation exposure of the aircrew and frequent flyers is higher. Additionally, it is noted that the difference among the values of the three FLs is larger towards lower rigidities, i.e., polar regions, and reduces towards higher rigidities, i.e., equatorial regions. Specifically, regarding the CRII, it is observed that during all phases of solar cycle 23, the values were smaller than those of the respective phases of solar cycle 24, eventuated from the fact that solar cycle 23 was very active whereas solar cycle 24 was a quiet one. Nonetheless, as one reaches equatorial regions, this difference becomes very small, which indicates that mostly low-rigidity regions are affected by solar activity.

KIEL-UP • DOI: 10.38072/2748-3150/p38

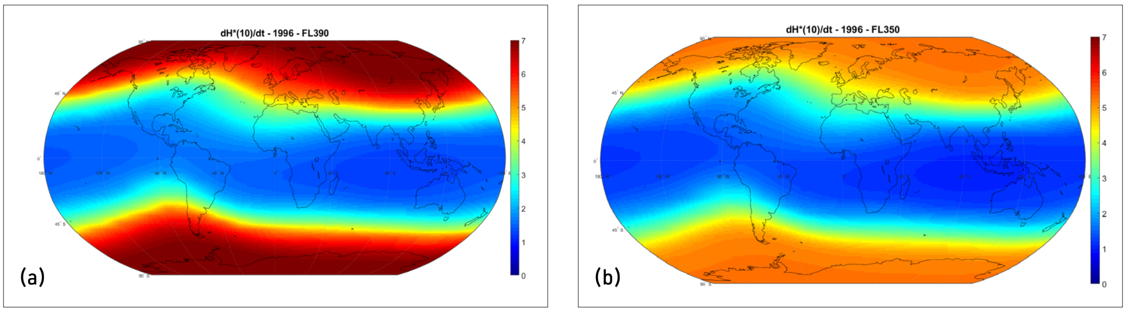

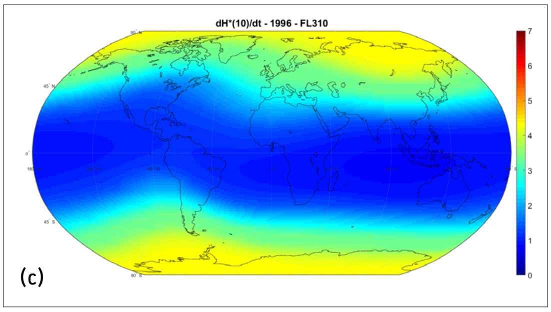

Fig. 4: Maps of the estimated ambient dose equivalent rate (μSv/h) during the minimum of solar cycle 23 (year 2001) at: (a) FL390; (b) FL350; (c) FL310.

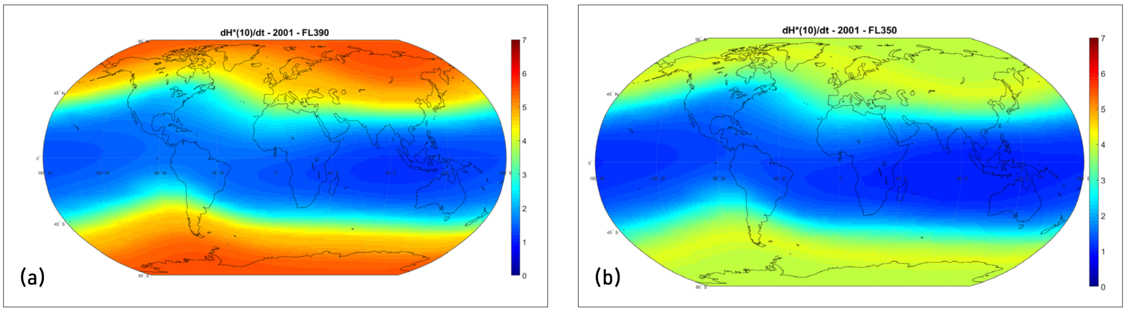

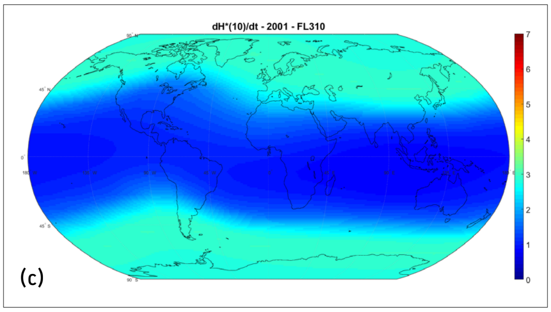

Fig. 5: Maps of the estimated ambient dose equivalent rate (μSv/h) during the maximum of solar cycle 23 (year 2001) at: (a) FL390; (b) FL350; (c) FL310.

The correlation between the annual distribution of the CRII and the dH*(10)/dt for all four rigidities mentioned before, for all three FLs, from 1996 to 2019, is illustrated in Figure 7. We observe a positive correlation between these two physical quantities, with a correlation coefficient of R^2=0.97. This confirms the contribution of CRII to the radiation deposited at different locations and altitudes.

KIEL-UP • DOI: 10.38072/2748-3150/p38

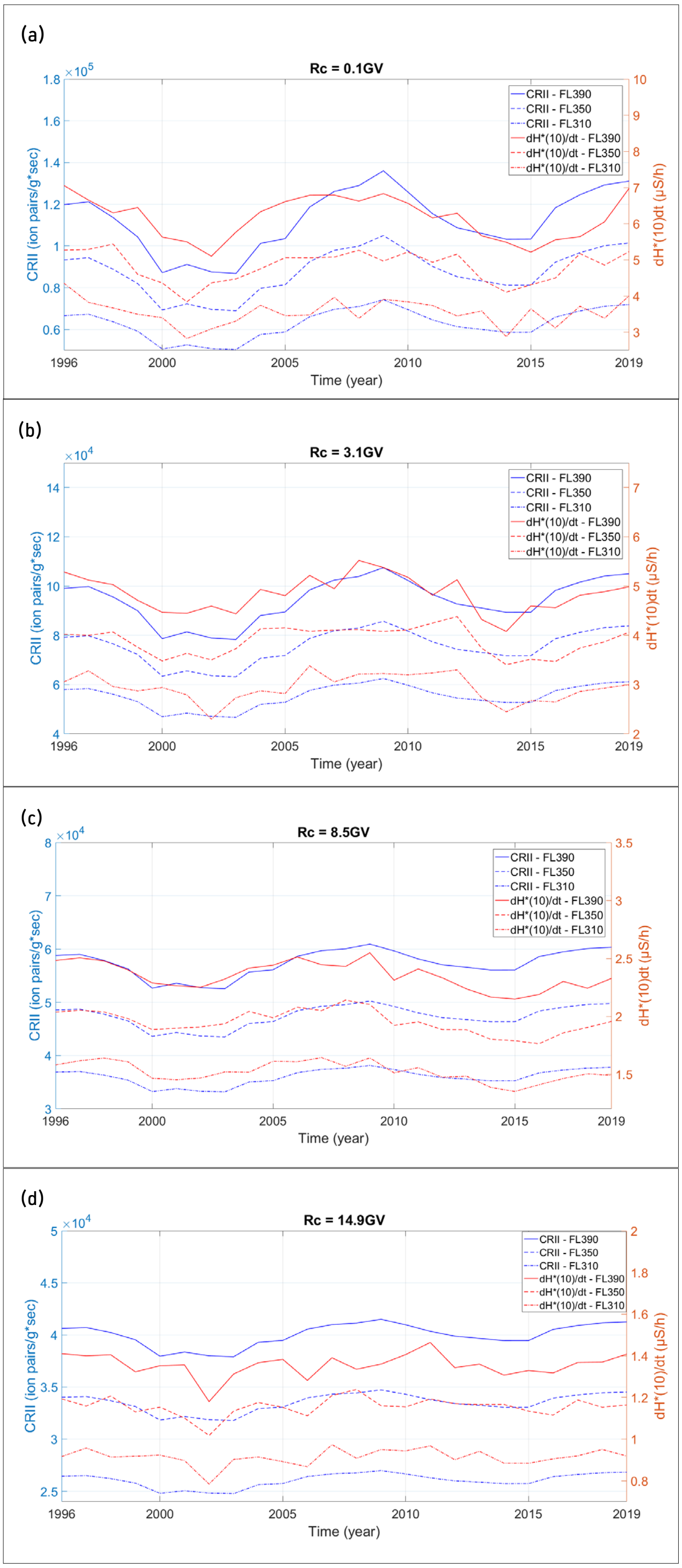

Fig. 6: Annual distribution of the CRII rate (left axis, blue lines) and ambient dose equivalent rate (right axis, red lines) at three different flight levels (FL310, FL350, FL390), during solar cycles 23 and 24 (years 1996–2019): (a) at a polar region with cut-off rigidity 0.1 GV; (b) a region with cut-off rigidity 3.1 GV; (c) at a region with cut-off rigidity 8.5 GV (Athens); (d) an equatorial region with cut-off rigidity 14.9 GV.

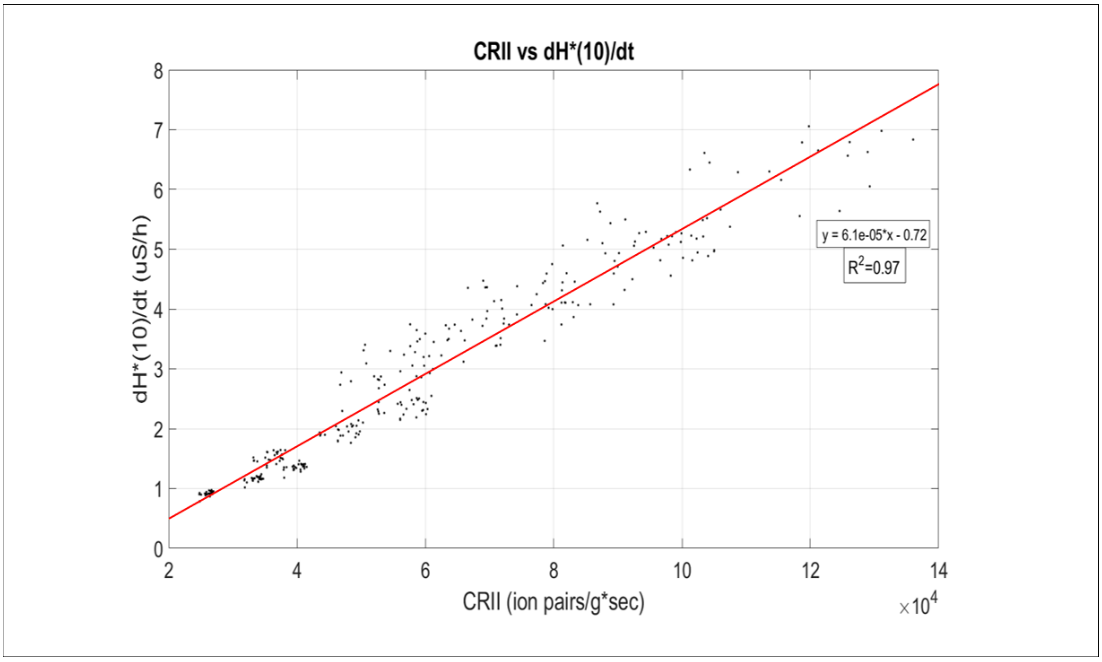

Fig. 7: Scatter plot of the annual distribution of the CRII rate and the ambient dose equivalent rate for the time period 1996–2019 at FL390, FL350, FL310.

4. Discussion and conclusions

Concluding, CRII and dH*(10)/dt follow the behavior of the cosmic ray intensity and are negatively correlated with the solar activity. The maximum values are observed during the solar minima and at polar regions (~ 7 µSv/h at FL390, 5 µSv/h at FL350 and 4 µSv/h at FL310), while the minimum values during the solar maxima and at the equatorial regions (~ 1.2 µSv/h at FL390, 1 µSv/h at FL350 and 0.8 µSv/h at FL310). It is observed that the higher the flight level, the higher the CRII and the radiation exposure of aircrew and frequent flyers, since the provided shielding of the atmosphere is reduced in higher atmospheric altitudes. Finally, comparing the CRII and dH*(10)/dt calculations the correlation is positive ($R^2 = 0.97$).

The CRAC:CRII and DYASTIMA tools are reliable and give useful results for the study of the impact of the ionization and radiation induced by cosmic rays on the environment, space weather, climate change (Dorman 2016; Todd and Kniveton 2001) and human health (Singh et al. 2011; Meier et al. 2020). As the number of flights keeps increasing and air traffic is elevated, commercial aircraft are forced to fly at higher flight levels, which leads to a variation of the CRII and the radiation exposure, according to the flight route and the FLs chosen during each flight. This field of research could be very useful to the aviation industry for updating safety measures and regulations, as well as the air traffic flow and capacity management.

Acknowledgements

This work is supported by the ESA Space Safety Programme's network of space weather service development and pre-operational activities, under ESA Contract 4000134036/21/D/MRP, in the context of the

KIEL-UP • DOI: 10.38072/2748-3150/p38

Space Radiation Expert Service Centre. I.G.U. acknowledges partial support from the Academy of Finland (projects ESPERIA No. 321882). Thanks are due to the Special Research Account of the University of Athens for supporting the Cosmic Ray research. Thanks are also due to the Oulu Cosmic ray colleagues for kindly providing cosmic ray data as well as the CRAC:CRII model.

Questions and answers

Question 1: How does your evaluation of radiation dose rates compare with those of commonly used models as EPCARD?
Answer: The comparison of radiation dose rates values with some other models (for example, CARI-7) has been performed indicatively during the validation process of the DYASTIMA-R tool. We have not yet performed a comparison with the results of EPCARD. Details about the validation process and the results (not the comparison with other models) may be found in Tezari A., Paschalis P., Mavromichalaki H., Karaiskos P., Crosby N., and Dierckxsens M. at Oxford Academic Journal Radiation Protection Dosimetry (https://dx.doi.org/10.1093/rpd/ncaa112).
Question 2: How did you calculate the CR fluxes arriving at the upper atmosphere at all locations on Earth?
Answer: Concerning the CRAC:CRII model, the differential energy spectrum of galactic cosmic rays is parameterized by the force field model which has only one parameter, the modulation potential , for a given local interstellar spectrum. Full details may be found at Usoskin and Kovaltsov (2006) and Usoskin et al. (2005, 2010, 2011). Concerning the DYASTIMA software, the differential spectrum of the incoming primary galactic cosmic rays at the top of the atmosphere, we used the ISO15390 model (ISO 15390:2004ISO, 2004).
Question 3: Do you have an idea how strong a GLE must be to give a significant signal in your models?
Answer: We haven't worked on GLEs yet.

References

Agostinelli, S.; Allison, J.; Amako, K.A.; Apostolakis, J.; Araujo, H.; Arce, P.; Asai, M.; Axen, D.; Banerjee, S.; Barrand, G.; et al. 2003, Geant4–A simulation toolkit. Nucl. Instrum. Methods A, 506(3), 250–303, http://doi.org/10.1016/S0168-9002(03)01368-8

Allison, J.; Amako, K.; Apostolakis, J.; Araujo, H.; Dubois, P.A.; Asai, M.; Barrand, G.; Capra, R.; Chauvie, S.; Chytracek, R.; et al. 2006, Geant4 developments and applications. IEEE Trans. Nucl. Sci., 53(1), 270–278, http://doi.org/10.1109/TNS.2006.869826

Allison, J.; Amako, K.; Apostolakis, J.; Arce, P.; Asai, M.; Aso, T.; Bagli, E.; Bagulya, A.; Banerjee, S.; Barrand, G.; et al. 2016, Recent developments in Geant4. Nucl. Instrum. Methods A, 835, 186–225, http://doi.org/10.1016/j.nima.2016.06.125

Athens Cosmic Ray Group, 2019, DYASTIMA Software User Manual, http://cosray.phys.uoa.gr/index.php/dyastima (last accessed July 5, 2023)

Bazilevskaya, G.A.; Usoskin, I.G.; Flückiger, E.O.; et al. 2008, Cosmic Ray Induced Ion Production in the Atmosphere. Space Sci Rev, 137, 149–173, https://doi.org/10.1007/s11214-008-9339-y

Berger, T., Meier, M., Reitz, G. and Schridde, M. 2008, Longterm dose measurements applying a human anthropomorphic phantom onboard an aircraft. Radiat. Meas., 43(2-6), 580–584, https://doi.org/10.1016/j.radmeas.2007.12.004

Dorman, L. I. 2016, Space Weather and Cosmic Ray Effects, Chapter 30, Climate Change, 513-544, https://doi.org/10.1016/B978-0-444-63524-2.00030-0

ESA https://swe.ssa.esa.int/dyastima-federated (last accessed July 5, 2023).

ESA 2019, ESA SSA P3 SWE-III Acceptance Test Report, R.137 Dynamic Atmospheric Tracking Interactive Model Application (DYASTIMA); ESA: Paris, France.

Flückiger, E. and Bütikofer, R. 2011, Radiation doses along selected flight profiles during two extreme solar cosmic ray events. Astrophys. Space Sci. Trans., 7(2), 105–109, https://doi.org/10.5194/astra-7-105-2011

Forbush, S. E. 1954, World wide cosmic ray variations, 1937–1952, J. Geophys. Res., 59(4), 525-542, https://doi.org/10.1029/JZ059i004p00525

Gerontidou, M.; Katzourakis, N.; Mavromichalaki, H.; Yanke, V.; Eroshenko, E. 2021, World grid of cosmic ray vertical cut-off rigidity for the last decade. Adv. Space Res., 67(7), 2231–2240. http://doi.org/10.1016/j.asr.2021.01.011

Gleeson, L. J. and Axford, W. I. 1968, Solar Modulation of Galactic Cosmic Rays. Astrophysical J., 154, 1011-1026, https://doi.org/10.1086/149822

International Commission on Radiation Units and Measurements 2010, Reference data for the validation of doses from cosmic-radiation exposure of aircraft crew. ICRU Report 84. J. Int. Comm. Radiat. Units Meas., 10.

International Commission on Radiological Protection 2007, The Recommendations of the International Commission on Radiological Protection. Ann. ICRP, 37, 103.

International Commission on Radiological Protection 2016, Radiological protection from cosmic radiation in aviation. Ann. ICRP, 45, 132.

ISO 2533:1975ISO Standard Atmosphere, International Organization for Standardization: Geneva, Switzerland, 2007.

ISO 15390:2004ISO Space Environment (Natural and Artificial)—Galactic Cosmic Ray Model, International Organization for Standardization: Geneva, Switzerland, 2004.

Makrantoni, P.; Mavromichalaki, H.; Usoskin, I. G.; Papaioannou, A. 2013, Calculation of the cosmic ray induced ionization for the region of Athens, J. Physics, Conf. Series 409, 2232, http://doi.org/10.1088/1742-6596/409/1/012232

Makrantoni, P.; Mavromichalaki, H.; Paschalis, P. 2021, Solar cycle variation of the ionization by cosmic rays in the atmosphere at the mid-latitude region of Athens, Astrophys. Space Sci., 366:70 https://doi.org/10.1007/s10509-021-03978-8

Makrantoni, P.; Tezari, A.; Stassinakis, A.N.; Paschalis, P.; Gerontidou, M.; Karaiskos, P.; Georgakilas, A.G.; Mavromichalaki, H.; Usoskin, I.G.; Crosby, N.; et al. 2022, Estimation of Cosmic-Ray-Induced Atmospheric Ionization and Radiation at Commercial Aviation Flight Altitudes. Appl. Sci., 12(11), 5297, https://doi.org/10.3390/app12115297

Mavromichalaki, H.; Marmatsouri, L.; Vassilaki, A. 1995, On reproduction of long term cosmic-ray modulation as seen by neutron monitor stations, Astrophys. and Space Sci., 232, 315-326, https://doi.org/10.1007/BF00658302

Mavromichalaki, H.; Belehaki, A.; Rafios, X. 1998, Simulated effects at neutron monitor energies: evidence for a 22-year cosmic-ray variation. Astron. Astrophys., 330, 764–772.

Meier, M.M.; Copeland, K.; Kloble, K.E.J.; Matthia, D.; Plettenberg, M.C.; Schennetten, K.; Wirtz, M.; Hellweg, C.E. 2020, Radiation in the atmosphere. A hazard to aviation safety? Atmosphere, 11(12), 1358. http://doi.org/10.3390/atmos11121358

National Oceanic and Atmospheric Administration, https://www.ngdc.noaa.gov/geomag/ (last accessed July 5, 2023)

OMERE, http://www.trad.fr/en/space/omere-software/ (last accessed July 5, 2023)

Paschalis, P.; Mavromichalaki, H.; Dorman, L.I.; Plainaki, C.; Tsirigkas, D. 2014, Geant4 software application for the simulation of cosmic ray showers in the Earth's atmosphere. New Astron., 33, 26–37, https://doi.org/10.1016/j.newast.2014.04.009

Singh, A.K.; Singh, D.; Singh, R.P. 2011, Impact of galactic cosmic rays on earth's atmosphere and human health. Atmos. Environ. 2011, 45(23), 3806–3818, http://doi.org/10.1016/j.atmosenv.2011.04.027

Smart, D.F.; Shea, M.A. 2007a, World grid of calculated cosmic ray vertical cutoff rigidities for epoch 1995.0. In Proceedings of the 30th International Cosmic Ray Conference, Yucatán, Mexico, 3–11 July.

Smart, D.F.; Shea, M.A. 2007b, World grid of calculated cosmic ray vertical cutoff rigidities for epoch 2000.0. In Proceedings of the 30th International Cosmic Ray Conference, Yucatán, Mexico, 3–11 July.

Smart, D.F.; Shea, M.A. 2019, Vertical Geomagnetic Cutoff Rigidities for Epoch 2015. In Proceedings of the 36th International Cosmic Ray Conference, Madison, WI, USA, 24 July –1 Aug.

Tezari, A.; Paschalis, P.; Mavromichalaki, H.; Karaiskos, P.; Crosby, N.; Dierckxsens, M. 2020, Assessing Radiation Exposure Inside The Earth's Atmosphere. Radiat. Prot. Dos., 190(4), 427–436, https://doi.org/10.1093/rpd/ncaa112

Tezari, A.; Paschalis, P.; Stassinakis, A.; Mavromichalaki, H.; Karaiskos, P.; Gerontidou, M.; Alexandridis, D.; Kanellakopoulos, A.; Crosby, N.; Dierckxsens, M. 2022, Radiation Exposure in the Lower Atmosphere during Different Periods of Solar Activity. Atmosphere, 13(2), 166, https://doi.org/10.3390/atmos13020166

Todd, M.C.; Kniveton, D.R. 2001, Changes in cloud cover associated with Forbush decreases of galactic cosmic rays. J. Geophys. Res., 106(D23), 32031–32042, http://doi.org/10.1029/2001JD000405

Usoskin, I.G.; Alanko-Huotari, K.; Kovaltsov, G.A.; Mursula, K. 2005, Heliospheric modulation of cosmic rays: Monthly reconstruction for 1951–2004. J. Geophys. Res., 110, A12108, http://doi.org/10.1029/2005JA011250

KIEL-UP • DOI: 10.38072/2748-3150/p38

Usoskin, I.G.; Kovaltsov, G.A. 2006, Cosmic ray induced ionization in the atmosphere: Full modeling and practical applications. J. Geophys. Res., 111, D21206, http://doi.org/10.1029/2006JD007150

Usoskin, I.G.; Desorgher, L.; Velinov, P.; Storini, M.; Flueckiger, E.O.; Buetikofer, R.; Kovaltsov, G.A. 2009, Ionization of the Earth's atmosphere by solar and galactic cosmic rays. Acta Geophys., 57, 88-101, http://doi.org/10.2478/s11600-008-0019-9

Usoskin, I.G.; Kovaltsov, G.A.; Mironova, I.A. 2010, Cosmic ray induced ionization model CRAC: CRII: An extension to the upper atmosphere. J. Geophys. Res., 115, D10302. http://doi.org/10.1029/2009JD013142

Usoskin, I. G.; Bazilevskaya, G. A.; Kovaltsov, G. A. 2011, Solar modulation parameter for cosmic rays since 1936 reconstructed from ground-based neutron monitors and ionization chambers, J. Geophys. Res., 116, A02104, http://doi.org/10.1029/2010JA016105

Open Access